applied sciences

MDPI

Article

Study on Creep Behavior of Silty Clay Based on Fractal Derivative

Qian Yin [1,2], Junping Dai [3], Guoliang Dai [1,2,*], Weiming Gong [1,2], Fan Zhang [1,2] and Mingxing Zhu [4]

[1] Key Laboratory of C&PC Structures, Ministry of Education, Southeast University, Nanjing 211189, China
[2] School of Civil Engineering, Southeast University, Nanjing 211189, China
[3] Jiangsu Provincial Transportation Engineering Construction Bureau, Nanjing 210004, China
[4] School of Civil Engineering and Architecture, Jiangsu University of Science and Technology, Zhenjiang 212100, China
* Correspondence: daigl@seu.edu.cn

Abstract: Soft soil is widely distributed in the riverside area of southern China. The creep deformation characteristics of the soft soil affect the long-term stability of the structure foundation, which cannot be ignored. Through the triaxial drainage creep test, the creep characteristics of riverside soil with a soft interlayer from Jiangsu Province were studied. The test results show that the creep procedure of the soft soil is divided into two stages, exhibiting steady-state creep and shear shrinkage characteristics with time and stress growth, which presents typical nonlinear behavior. Additionally, the confining pressure and stress are critical factors affecting creep characteristics. The fractal dashpot based on fractal derivative theory is introduced in place of the Abel dashpot in the classical fractional Burgers model; a fractal Burgers creep model with few parameters, high precision, and clear physical significance is established. Additionally, an analytical solution to the creep model is given. The model parameters are determined by fitting the test results, and the comparison shows that the results estimated with the model are more accurate than those estimated with the traditional model. The sensitivity analyses of the model parameters reveal the influence of key parameters on the creep characteristics of the soil. The results further confirm that the proposed fractal Burgers model can characterize the creep behavior of viscoelastic soil. These observations are extremely important for predicting the foundation displacement and formulating measures to prevent the deformation, which can provide a reference for engineering applications in the riverside area of southern China.

Keywords: silty clay; triaxial creep test; creep characteristics; fractal derivative; fractal Burgers model

Citation: Yin, Q.; Dai, J.; Dai, G.; Gong, W.; Zhang, F.; Zhu, M. Study on Creep Behavior of Silty Clay Based on Fractal Derivative. *Appl. Sci.* **2022**, *12*, 8327. https://doi.org/10.3390/app12168327

Academic Editor: Daniel Dias

Received: 28 June 2022
Accepted: 17 August 2022
Published: 20 August 2022

1. Introduction

In response to the call for national transportation power, the construction of several high-quality bridges to garner worldwide attention in China has gradually been put on the agenda. Zhangjinggao Yangtze River Bridge is a super long-span highway suspension bridge with a main span of 2300 m under construction in China, which is located in Jiangsu Province and crosses the Yangtze River, as shown in Figure 1. The bridge foundation by the riverside is situated in an area of strata with a deep silty clay interlayer and abundant pore water, as shown in Figure 2. This kind of soil usually has the characteristics of high moisture content, high compressibility, low shear strength, and low permeability, showing obvious creep characteristics of deformation with stress and time growth, which will affect the long-term stability of the bridge foundation. To effectively control the post-construction displacement of the foundation and ensure the long-term stable operation of the foundation, it is of great practical significance to study the creep characteristics of this soft soil interlayer.

Creep characteristics are one of the most important engineering properties of soft soil and represent the relationship between soil stress and strain with time. These characteristics of soil have an important impact on the stability and long-term operation of foundations.

Laboratory testing is an important method to investigate creep characteristics. The previous studies have mainly focused on direct shear creep tests [1,2], ring shear tests [3,4], uniaxial compression tests [5–7], and triaxial creep tests [8–10], to reveal the mechanism of soil and rock creep deformation. As far as theoretical analysis is concerned, the creep theory model of the relationship between soil deformation and time change is primarily established by a mathematical formula. At present, the commonly applied creep model can be divided into two types, the empirical and the element creep model. The empirical creep model, such as the Singh–Mitchell model and Mesri model [11,12], directly fits the creep relationship curve of the soil through the mathematical function, which is an empirical formula based on the regression analysis of the soil creep test results. It can describe the creep characteristics of the soil in a targeted manner but has the disadvantage of lacking a theoretical basis. Element creep model is a combination of ideal basic components with elasticity, plasticity, and viscosity, while the creep constitutive model is further derived according to the constitutive relationship of each component. There are several widely used models including the Maxwell model, the Kelvin model, the Bigham model, and the Nishihara model [13–15]. Hou et al. [16] established an improved Nishihara model that considered hardening variables and damage variables, which could excellently describe the creep characteristics of artificially frozen soil. Zhang et al. [17] proposed a creep model combined with Hook, Kalvin, and viscoplastic elements, which accurately characterized the creep behavior of mudstone. Ye et al. [18] established an improved nonlinear damage Burgers model to reflect the creep process of calcareous coral sand and verified its effectiveness. Tian et al. [19] proposed a damage creep model by combining the Maxwell element with the viscoplastic element and perfectly expressed the shear creep behavior of microbial improved expanded soil. The established model is helpful to understand the creep behavior, stress relaxation, and stable deformation of soil. Compared with the empirical model, the element creep model has the advantage of the flexible description of different creep behaviors. However, the complexity of the constitutive model makes the parameters difficult to determine.

Figure 1. Location of Zhangjinggao Yangtze River Bridge.

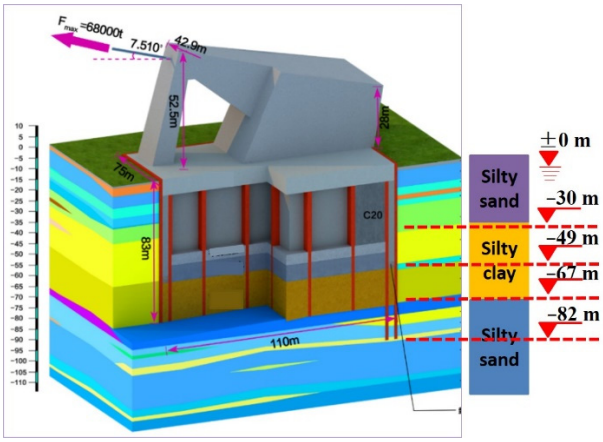

Figure 2. The geological condition of the south anchorage foundation.

The fractional creep model based on fractional calculus theory is able to achieve higher accuracy with fewer parameters in the simulation of the rheological phenomenon of materials [10,20,21], and is widely used to describe the viscoelastic behavior of concrete, rock, coal, and soil. Liang et al. [22] have well characterized the ultraslow creep process of self-compacting concrete by the fractional Maxwell model. Wu et al. [23] established a viscoelastic creep model of salt rock based on the theory of a fractional calculus operator and verified the reliability of the model in simulating the creep process of rock. On the basis of the Scott-Blair fractional order element and variable coefficient fractional order element, Su et al. [24] proposed a nonlinear variable-order fractional viscoelastic plastic creep model and extended the model to a three-dimensional situation, which well characterized the creep characteristics of deep coal. Liao et al. [25] established a fractional rheological element model of warm frozen silt and proposed a creep strength criterion by promoting a triaxial test. Zhang et al. [26] verified the validity of the proposed viscoelastic Kevin-V fractional derivative model based on the laboratory test of frozen sand. Xu et al. [20] described the time-dependent behavior of Shanghai marine clay through the improved fractional merchant model. However, compared with the integer derivative model, the development of global operators through convolution integration of fractional derivatives requires higher computing costs and memory requirements [27].

Therefore, the fractal theory, which evolved from the fractional theory, gradually developed because of its local operator without convolution integrals [27]. Compared with fractional derivative theory, fractal derivative theory can provide a higher calculation efficiency and fitting accuracy under the same number of parameters, which have been applied and promoted in many engineering fields [28–30], and gradually began to be applied in geotechnical engineering to characterize the rheological behavior of rock and soil materials. Cai et al. [27] first proposed the fractal Maxwell model and the fractal Kelvin model and confirmed the proposed fractal model could characterize the creep behavior of viscoelastic frozen soil. Su et al. [31] applied Hausdorff's fractal derivative to establish the fractal Bingham model to describe the viscoelastic deformation characteristics and verified the accuracy of the proposed fractal model by fitting the relevant rheological test data. Wang et al. [32] proposed a time fractal derivative constitutive model to describe the whole creep region of granite by replacing the Newton dashpot with a fractal dashpot. Yao et al. [33] introduced an unsteady fractal derivative creep model to describe a soft interlayer's complete creep failure process. Kabwe et al. [34] proposed a fractal derivative viscoelastic and viscoplastic constitutive model with isotropic damage to describe the creep mechanism and mean deformation in squeezing ground reasonably well. Gao et al. [35] suggested a fractal merchant model that characterizes the creep behavior of marine-terrestrial deposit soil, which obtained satisfactory results, demonstrating that the fractal derivative theory is appropriate to describe the creep characteristics of the soil.

In general, the fractal derivative theory has been verified in several fields with high computational efficiency and the ability to characterize the creep of materials. However, there have been few reports on the fractal derivative creep model of geotechnical materials at present. It is not clear whether the fractal derivative creep model can be used to characterize the creep characteristics of silty clay in riverside areas of south China. Based on the above considerations, a triaxial drainage creep test was carried out to study the creep characteristics of the undisturbed silty clay samples along the Yangtze River in Jiangsu Province. By introducing fractal derivative theory, an improved fractal derivative Burgers model is proposed to describe the creep behavior of silty clay with fewer parameters and higher accuracy. The research results can be used to predict the displacement of the foundation and formulate measures to control the deformation, which provide a reference value for the creep characteristics of riverside soft soil in southern China.

2. Test Procedure and Results

2.1. Soil Properties

The South Anchorage Foundation of Zhangjinggao Yangtze River Bridge is located in Zhangjiagang, Jiangsu Province. The soil within the buried depth of the foundation is mainly silty sand, but there is a silty clay soil interlayer with a thickness of 20~37 m below −30 m, as shown in Figure 3. The creep characteristic of this layer of soft soil is a crucial factor affecting the long-term deformation of the bridge foundation. To study the creep characteristics of the soft soil interlayer, a series of laboratory triaxial drained creep tests of this layer of undisturbed soil was carried out. The soil samples were obtained from 55 m-deep boreholes drilled by the Yangtze River in Zhangjiagang, sealed on site, and transported to the laboratory for storage under constant temperature and humidity. Their basic physical and mechanical property indexes are shown in Table 1 and Figure 4. The soil is defined as flow-plastic silty clay with reference to the Chinese code [36].

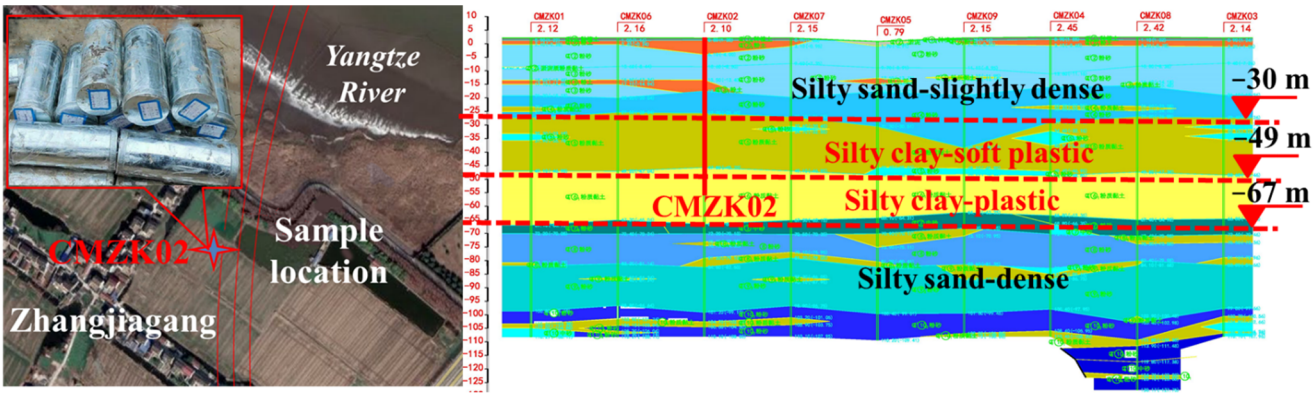

Figure 3. Location of the soil sample.

Table 1. Physical and mechanical properties of the test soil.

Depth (m)	Water Content ω (%)	Unit Weight γ (kN/m^3)	Liquid Limit ω_L (%)	Plasticity Index I_p (%)
50~55	35.4	18.6	37.5	14.8

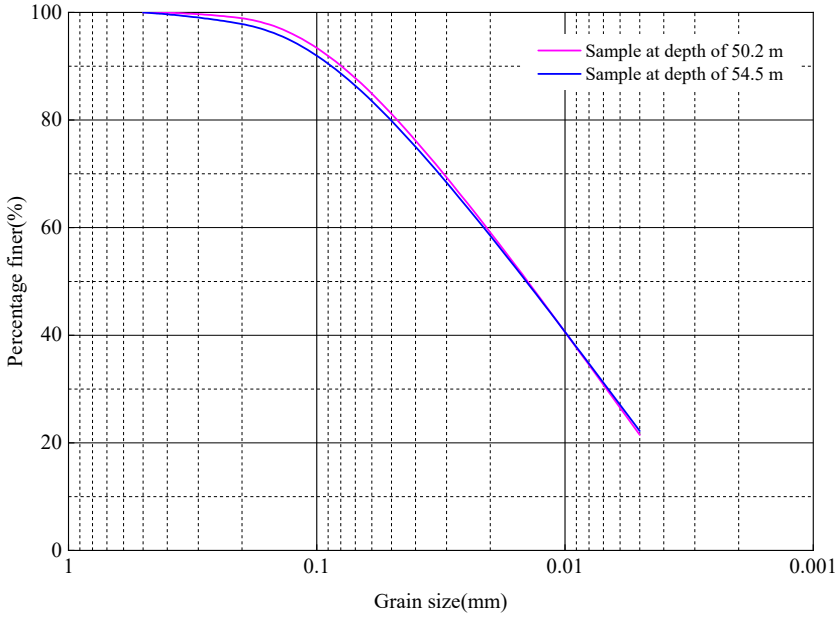

Figure 4. Gradation curve of the soil sample.

2.2. Test Procedure

The triaxial consolidation drained tests were carried out by the TSZ automatic triaxial apparatus, and the diameter and height of the samples were 39.1 mm and 80 mm, respectively. The temperature was controlled to 20 ± 1 °C during the test, and a series of various eccentric stress were applied to different samples separately. Compared with applying a graded loading, this method can directly obtain the soil creep test data and avoid manual processing errors to reflect the creep characteristics of soil more accurately. To obtain the failure deviatoric stress of $q_f = (\sigma_1 - \sigma_3)_f$ under different confining pressures σ_3, a series of triaxial consolidated drained shear (CD) tests were carried out at four levels, the shear rate was set as 0.01%/min, and the test was performed in accordance with Chinese standards [37]. The obtained shear strength indexes (effective cohesion c' and effective friction angle φ') are shown in Table 2, and the results are shown in Figure 5. The failure deviatoric stress q_f was divided into 5 levels, the loading increment of each level was $\Delta q = q_f/5$, and the creep characteristics of sample soils below the failure deviatoric stress levels q were researched through a triaxial consolidated drained creep test. The samples were consolidated under the target confining pressure for 30 h prior to the test, respectively. Then, the axial loads were imposed on the samples until the target deviatoric stress q was reached. Finally, the stress was kept constant with a precision of ±10 kPa and the creep behavior was observed. At present, there are no standardized creep stability criteria; Sun [14] suggests that the general total observation time is set to 7~14 d in the case of the deformation reaching the stabilization stage or the constant strain rate stage. In this paper, the test was terminated after the observation time of the deformation stabilization stage reached 7 d, and the cumulative creep deformation of one consecutive 24 h period was lower than 0.01 mm [14]. The testing procedure was performed in accordance with Yuan et al. [38], and the data were automatically collected by the acquisition system of the instrument. The loading application scheme is shown in Table 3.

Table 2. The triaxial consolidated drained shear test program.

Test No.	σ_3 (kPa)	q_f (kPa)	c' (kPa)	φ' (°)
1	100	288	12.4	33.7
2	200	568		
3	300	836		
4	400	1057		

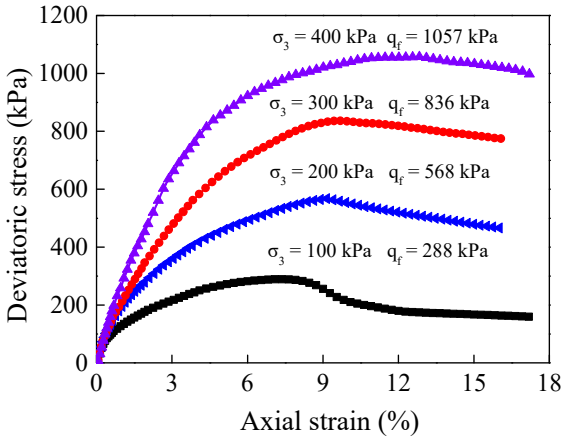

Figure 5. Stress-strain curves of the silty clay samples in the CD triaxial test.

Table 3. Loading application scheme of the triaxial creep test.

Test No.	σ_3 (kPa)	q_f (kPa)	q (kPa)	Test Time (h)
1	100	288	57	170
2			116	190
3			169	190
4			243	170
5	200	568	117	170
6			220	170
7			330	170
8			459	170
9	400	1057	197	170
10			422	170
11			617	170
12			863	170

2.3. Test Results and Analysis

The creep curves of the shear strain versus the time of undisturbed silty clay under different stress states and confining pressures were obtained through the triaxial creep tests, as shown in Figure 6. The corresponding relations of the creep strain rate versus time are shown in Figure 7 (taking the confining pressure of 200 kPa and the approximately deviatoric stress of 200 kPa as an example). Figures 6 and 7 show that the instantaneous and total strain of the soil is more significant when the confining pressure is low, indicating that the higher confining pressure can improve the instantaneous stiffness of the soil. Additionally, as the soil gradually consolidates, the creep deformation is also reduced. Furthermore, the creep deformation of the soil is mainly composed of instantaneous deformation, and the creep deformation characteristics under low stress is negligible but gradually become obvious when the stress increases. Nevertheless, the total creep deformation is relatively not significant and eventually tends to an asymptotic value by time, showing nonlinear characteristics. The creep strain rate also increases with the promotion of deviatoric stress, decreases with the increase in confining pressure, and gradually tends to be stable with time.

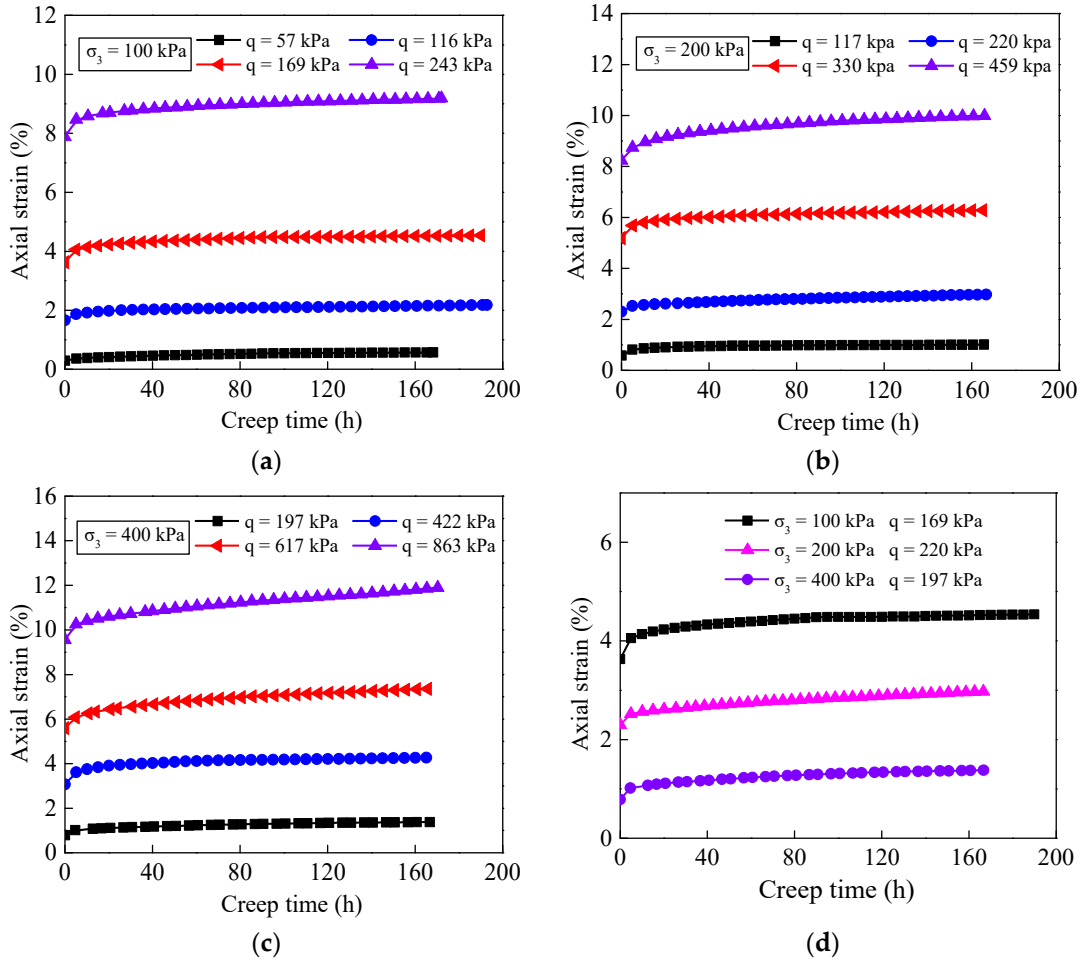

Figure 6. Relation of axial strain versus time under different confining pressures and stresses: (**a**) σ_3 = 100 kPa; (**b**) σ_3 = 200 kPa; (**c**) σ_3 = 400 kPa; (**d**) approximately q = 200 kPa.

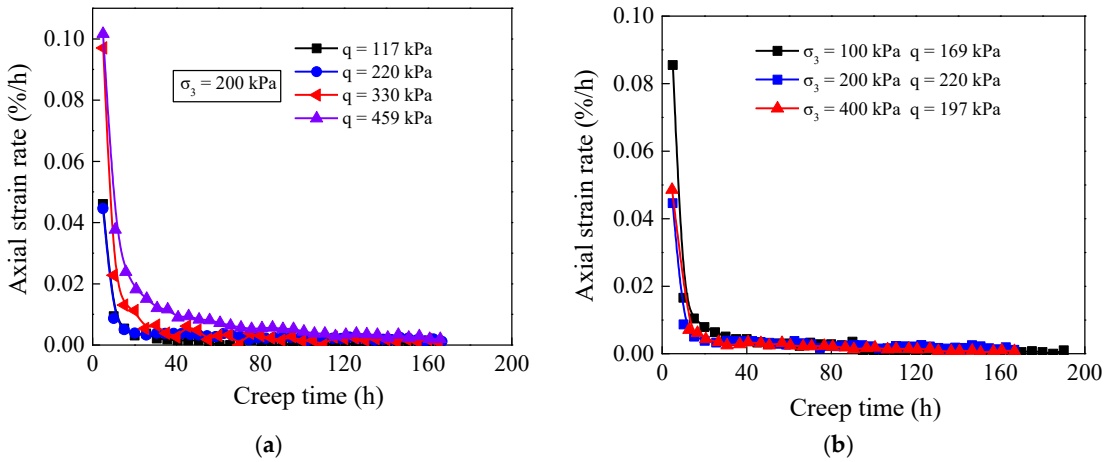

Figure 7. Relation of axial strain rate versus time: (**a**) σ_3 = 200 kPa; (**b**) approximately q = 200 kPa.

In general, the failure deviatoric stress increases with increasing confining pressure. Meanwhile, the deformation trends of soil under different confining pressures and deviatoric stresses are similar. In the case where the deviatoric stress loading value during the test is always lower than the failure level, the creep deformation presents the following two stages. In the initial transient creep stage, the creep deformation increases significantly,

accompanied by a remarkable change in creep rate. As time goes on, it gradually enters the steady-state creep stage, in which the creep rate tends to zero in the low-stress state or remains constant in the high-stress state, as is consistent with the findings of Gao [35] and Deng [39] in coastal soft soils in South China.

To further comprehend the creep characteristics of silty clay, the stress-strain isochronous curves of different confining pressures and deviatoric stresses are given as shown in Figure 8. The respective curves follow similar nonlinear trends under different deviatoric stress conditions and are related to the loading time. In addition, as the isochronous curves deviate from the straight line to a greater extent, the degree of nonlinearity becomes more obvious with increasing deviatoric stress and time. For the sample with constant deviator stress, the strain is negatively correlated with the change in confining pressure, which illustrates that the creep behavior of soil is the result of the combined action of time, stress, and confining pressure.

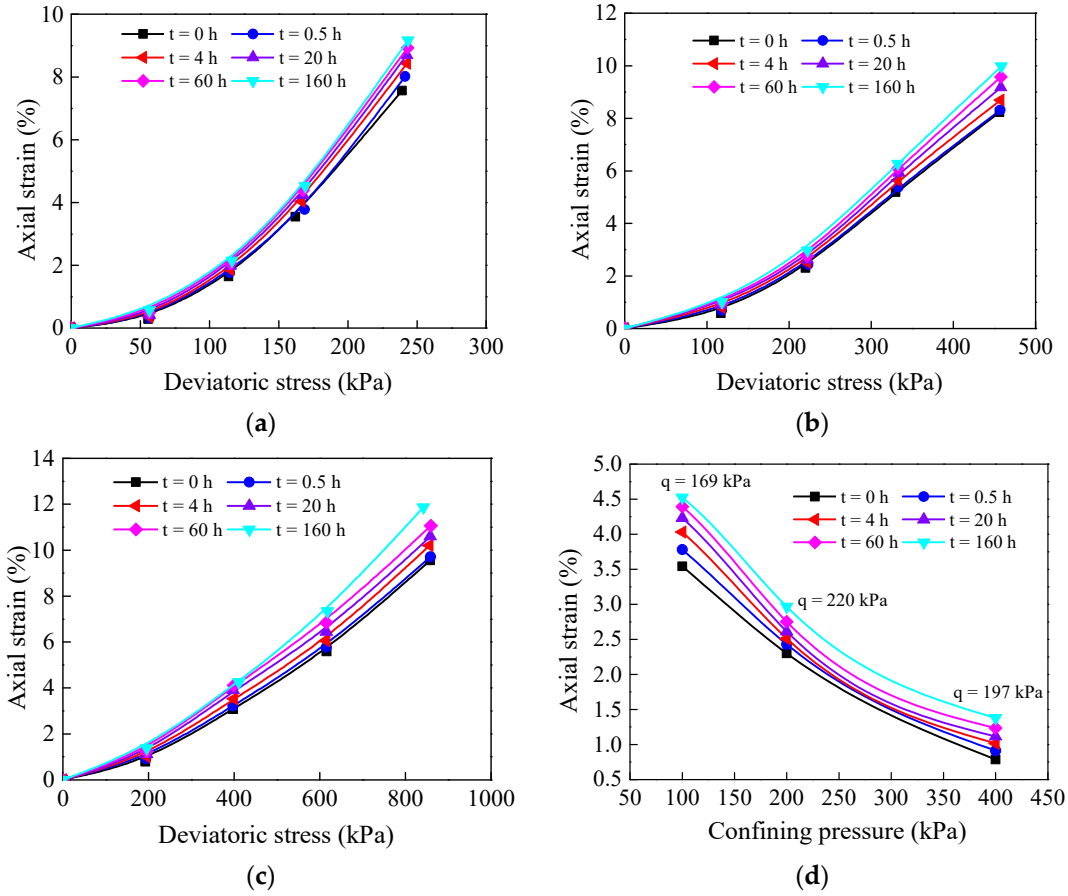

Figure 8. Isochronous curves of axial strain under different confining pressures and stresses: (**a**) σ_3 = 100 kPa; (**b**) σ_3 = 200 kPa; (**c**) σ_3 = 400 kPa; (**d**) approximately q = 200 kPa.

Figure 9 shows the relation of volumetric strain versus time under different confining pressures and deviatoric stresses. Figure 10 is the relation of volumetric strain rate versus time (taking the confining pressure of 200 kPa and the approximately deviatoric stress of 200 kPa as an example). It can be seen that, as time goes on, the volume strain rate is decreasing, and the volume strain shows an increasing trend, which is showing instability behavior. Similar to the axial strain changing tendency, the volumetric strain decreases gradually with the increase of the time and deviatoric stress, indicating that the soil displays shear contraction behavior, which differs from the volumetric deformation changing mode of Zhanjiang strong structured clay [40]. It is possibly caused by the differences in consolidation state, stress history, and stress level [41]. In addition, regional differences also lead to particle compositions and basic mechanical properties of soil in distinguishing.

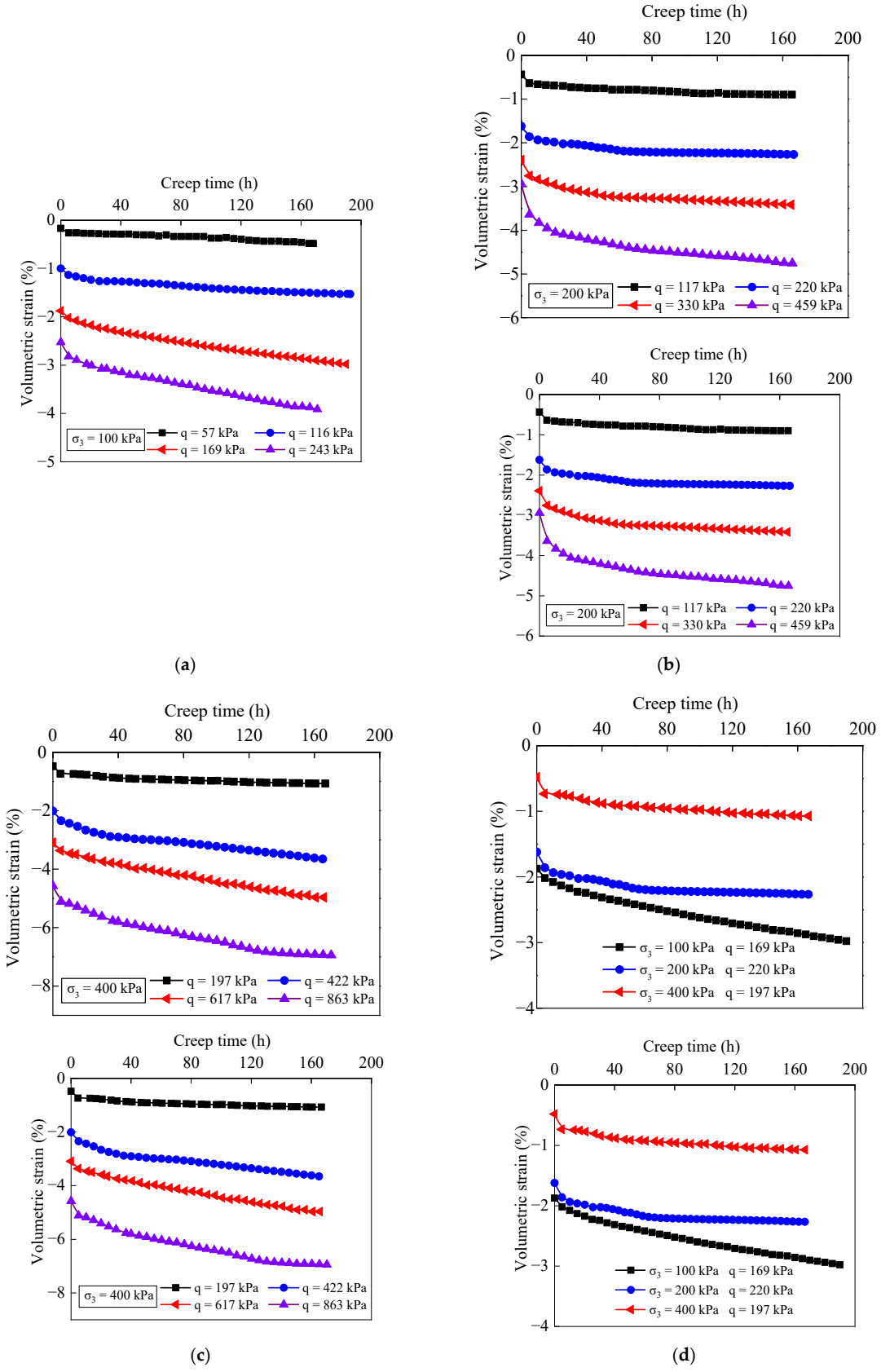

Figure 9. Relation of volumetric strain versus time under different confining pressures and stresses: (**a**) σ_3 = 100 kPa; (**b**) σ_3 = 200 kPa; (**c**) σ_3 = 400 kPa; (**d**) approximately q = 200 kPa.

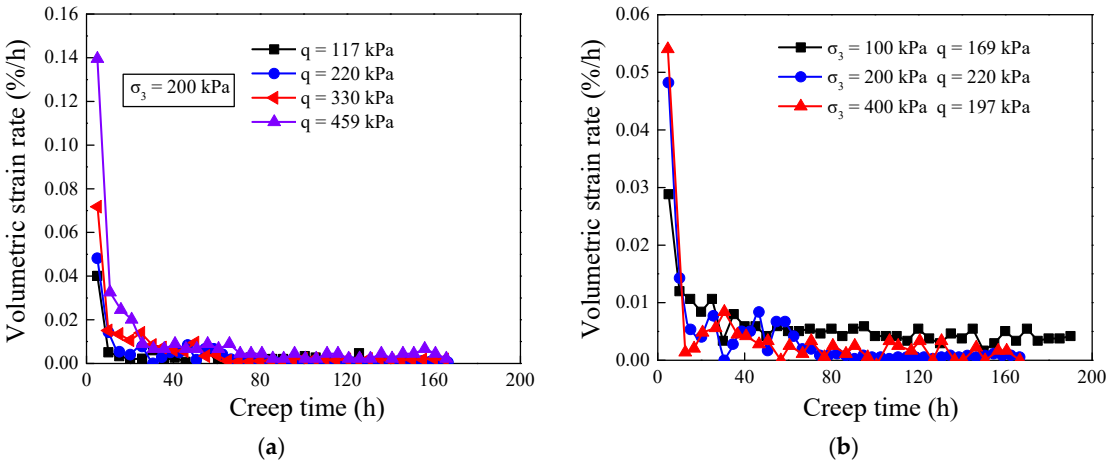

Figure 10. Relation of volumetric strain rate versus time: (**a**) σ_3 = 200 kPa; (**b**) approximately q = 200 kPa.

3. Fractal Creep Model

3.1. Basic Theory of the Fractal Derivative

The fractal derivative of time can be expressed as follows by transforming standard integer time into fractal time formation [27]:

$$\frac{df(t)}{dt^\beta} = \lim_{t_0 \to t} \frac{f(t) - f(t_0)}{t^\beta - t_0^\beta}, 0 < \beta \tag{1}$$

where β represents the fractal derivative order of time t. The significant difference in the definitions of the fractal and fractional derivatives is that the fractal derivative is a local operator [30]. According to the assumption of fractal invariance and equivalence, the fractal derivative can be transformed into classical derivative form through the scale transformation of $\hat{t} = t^\beta$.

3.2. Fractal Dashpot

The element model is widely used to describe the creep characteristics of soil because of its rigorous theoretical derivation process and explicit physical meaning of parameters, of which Hooke spring, Newton dashpot, and Abel dashpot elements are the most common. In recent years, to better represent the rheological properties of viscoelastic materials, Cai et al. [27] proposed an improved fractal dashpot to replace the Abel dashpot of fractional derivatives. The unified form of the constitutive equations and the corresponding stress-strain relationships for different models are formulated in Table 4, where η is Young's modulus or a viscosity coefficient, α and β denote the order of the derivative, and $\Gamma(\cdot)$ is the gamma function. It can be easily understood from the table that the fractal dashpot and Abel dashpot develop into a Hooke spring when $\alpha = \beta = 0$ and evolve into a Newton dashpot when $\alpha = \beta = 1$; between these endpoints, they exhibit viscoelastic material properties.

To compare the properties of the fractal dashpot and the Abel dashpot, the values σ = 100 kPa, η = 40 kPa·h$^\beta$, β = 0.4 were substituted into the constitutive model, respectively. The comparative analysis curves of the order β and viscosity coefficient η sensitivity of the Abel dashpot and fractal dashpot are shown in Figure 11a,b, which demonstrates that the fractal dashpot has nearly an equivalent effect as the Abel dashpot: the creep strain is positively correlated with the order and negatively correlated with the viscosity coefficient. The order and viscosity coefficient can appropriately describe the viscoelastic deformation and attenuation rate of the material.

Table 4. Comparison of different component models.

	Hooke Spring	Newton Dashpot	Abel Dashpot	Fractal Dashpot
Symbol		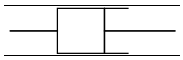	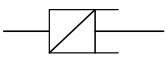	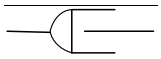
Constitutive modelRelations	$\sigma(t) = \eta \frac{d^{\alpha}\varepsilon(t)}{dt^{\beta}}$			
Relationship of stress and strain	$\varepsilon(t) = \frac{\sigma(t)}{\eta} t^{\beta}$	$\varepsilon(t) = \frac{\sigma(t)}{\eta} t^{\beta}$	$\varepsilon(t) = \frac{\sigma(t)}{\eta \cdot \Gamma(1+\beta)} t^{\beta}$	$\varepsilon(t) = \frac{\sigma(t)}{\eta} t^{\beta}$
The order value	$\alpha = \beta = 0$	$\alpha = \beta = 1$	$0 \leq \alpha = \beta \leq 1$	$\alpha = 1, 0 \leq \beta \leq 1$
Creep model	traditional model	traditional model	fractional model	fractal model

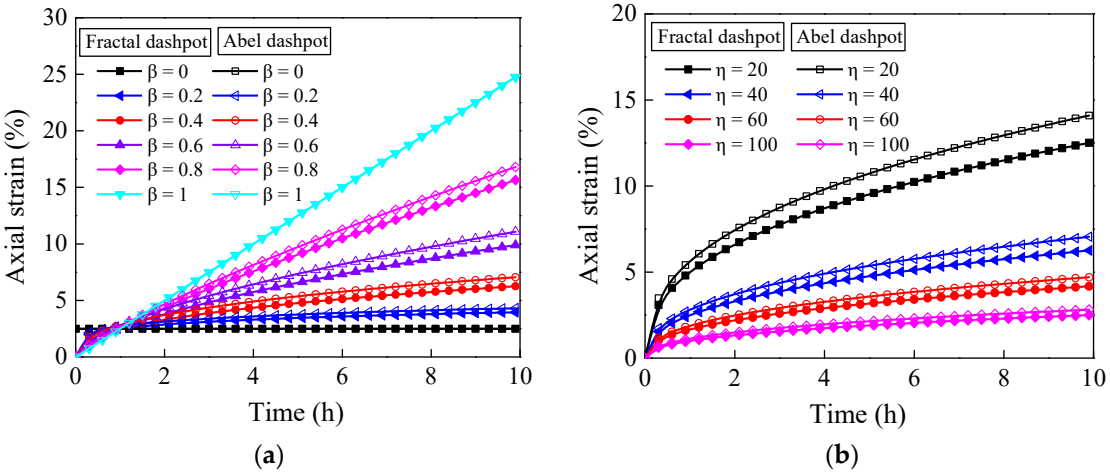

Figure 11. Sensitivity of the creep strain to the derivative order and viscosity coefficient: (**a**) σ =100 kPa and η = 40 kPa·h$^{\beta}$; (**b**) σ = 100 kPa and β = 0.4.

3.3. Fractal Burgers Model

The traditional Burgers model is composed of a Maxwell model and a Kelvin model in series, as shown in Figure 12a. The creep modulus of the traditional Burgers model is expressed as

$$J(t) = \frac{1}{E_m} + \frac{1}{\eta_m} t + \frac{1}{E_k}\left(1 - e^{-\frac{E_k}{\eta_k} t}\right) \tag{2}$$

where σ and ε are the stress and strain, E and η are Young's modulus and the viscosity coefficient, and the subscripts m and k represent Maxwell and Kelvin elements in a fractal form, respectively.

Since the typical traditional Burgers model is unable to exactly fit the initial stage of viscoelastic creep, the fractional Burgers model replacing the Newton dashpot with the Abel dashpot was proposed, as shown in Figure 12b. The Caputo fractional derivative theory can be expressed as [42]

$$\frac{d^{\beta} f(t)}{dt^{\beta}} = \frac{1}{\Gamma(n+1-\beta)} \int \frac{f^{(n+1)}(\tau)}{(t-\tau)^{(\beta-n)}} d\tau, n-1 \leq \beta < n \tag{3}$$

where β is the order of time fractal derivative, n represents a rational number, $\Gamma(\cdot)$ denotes the gamma function.

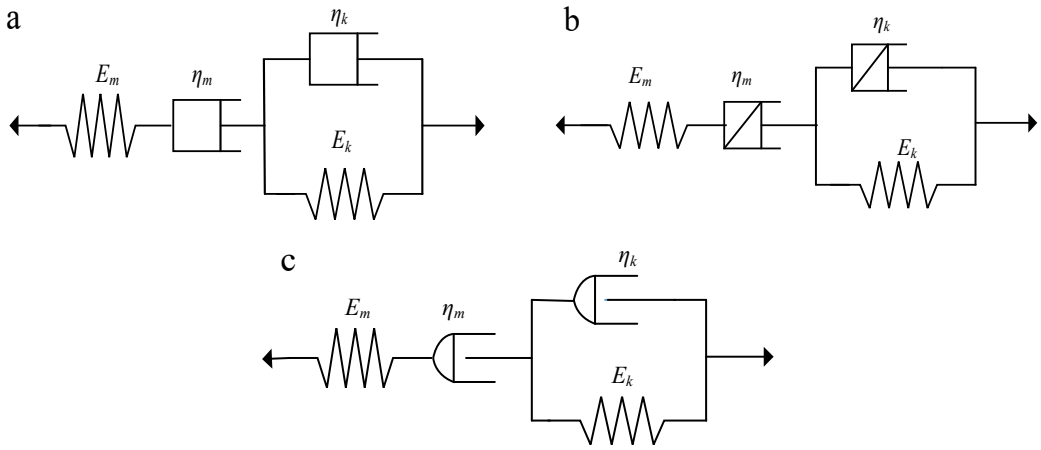

Figure 12. Schematic of different Burgers models: (**a**) Burgers model; (**b**) fractional Burgers model; (**c**) fractal Burgers model.

The fractional Burgers creep modulus based on Caputo fractional derivative theory can be expressed as [43]

$$J(t) = \frac{1}{E_m} + \frac{1}{\eta_m}\frac{t^\beta}{\Gamma(1+\beta)} + \frac{1}{E_k}\left[1 - E_\beta\left(-\left(\frac{t}{\eta_k}\right)^\beta\right)\right], 0 \le \beta \le 1 \tag{4}$$

where $E_\beta(\cdot)$ is a single-parameter Mittag-Leffler function proposed as [44]

$$E_\beta(x) = \sum_{n=0}^{\infty} \frac{x^n}{\Gamma(1+\beta n)}, \beta > 0 \tag{5}$$

This fractional derivative creep model can accurately fit the initial stage of viscoelastic creep and has been widely promoted and applied. However, it has the defect of the complex solution process of the fractional derivative convolution integral [45].

In this paper, we attempt to construct the fractal Burgers model by replacing the Abel dashpot with a fractal dashpot, as shown in Figure 12c. Under the premise of ensuring the accuracy of the simulated creep behavior, the calculation efficiency is improved by avoiding the local operator of convolutional integration.

According to the component element rules between Maxwell and Kelvin, the stress–strain relationship of the fractal Burgers model can be described as

$$\begin{cases} \varepsilon = \varepsilon_m + \varepsilon_k \\ \sigma = \sigma_m = \sigma_k \\ \frac{\sigma_m}{\eta_m} + \frac{1}{E_m}\frac{d\sigma_m}{dt^\beta} = \frac{d\varepsilon_m}{dt^\beta} \\ \frac{\sigma_k}{\eta_k} = \frac{E_k}{\eta_k}\varepsilon_k + \frac{d\varepsilon_k}{dt^\beta} \end{cases} \tag{6}$$

The constitutive relation is

$$\sigma + \left(\frac{\eta_m + \eta_k}{E_k} + \frac{\eta_m}{E_m}\right)\frac{d\sigma}{dt^\beta} + \frac{\eta_m\eta_k}{E_mE_k}\frac{d}{dt^\beta}\left(\frac{d\sigma}{dt^\beta}\right) = \eta_m\frac{d\varepsilon}{dt^\beta} + \frac{\eta_m\eta_k}{E_m}\frac{d}{dt^\beta}\left(\frac{d\varepsilon}{dt^\beta}\right) \tag{7}$$

By performing a Laplace transform on Equation (6), the following equation can be obtained

$$\begin{cases} \bar{\varepsilon} = \overline{\varepsilon_m} + \overline{\varepsilon_k} \\ \sigma = \sigma_m = \sigma_k \\ \frac{\sigma_m}{\eta_m s} + \frac{1}{E_m}\sigma_m = \overline{\varepsilon_m} \\ \frac{\sigma_k}{\eta_k s} - \frac{E_k}{\eta_k s}\overline{\varepsilon_k} = \overline{\varepsilon_m} \end{cases} \tag{8}$$

which can be simplified as

$$\bar{\varepsilon} = \left(\frac{1}{E_m} + \frac{1}{\eta_m s} + \frac{1}{E_k(1 + \frac{\eta_k}{E_k} s)} \right) \sigma \tag{9}$$

Through the time scale transformation of $\hat{t} = t^{\beta}$, and combined with the inverse Laplace transform, the fractal Burgers creep equation can be expressed as

$$\varepsilon(t) = \left[\frac{1}{E_m} + \frac{1}{\eta_m} t^{\beta} + \frac{1}{E_k} \left(1 - e^{-\frac{E_k}{\eta_k} t^{\beta}} \right) \right] \sigma_0 \tag{10}$$

The creep modulus of the fractal Burgers model is formulated by

$$J(t) = \frac{1}{E_m} + \frac{1}{\eta_m} t^{\beta} + \frac{1}{E_k} \left(1 - e^{-\frac{E_k}{\eta_k} t^{\beta}} \right) \tag{11}$$

4. Model Verification and Parametric Sensitivity Analysis

4.1. Fractal Burgers Model Verification

By fitting the test data according to the fractal Burgers model, as shown in Equation (10), with the least-squares method, the fractal Burgers model parameters under a confining pressure of 200 kPa are shown in Table 5. The test data and fitting curves of the fractal Burgers model and the fractional Burgers model are shown in Figure 13.

Table 5. Creep parameters of fractal Burgers model.

σ_3 (kPa)	q (kPa)	β	E_m (kPa)	η_m (kPa·h$^{\beta}$)	E_k (kPa)	η_k (kPa·h$^{\beta}$)	R^2
200	117	0.7	200	47483	347	1169	0.996
	220	0.7	96	16889	1026	1841	0.999
	330	0.4	64	5546	511	1045	0.999
	459	0.5	56	18917	266	1872	0.999

Figure 13 shows that both the fractal Burgers model and the fractional Burgers model effectively describe the triaxial creep characteristics of the first two stages of the soil under low deviatoric stress, while the fractal Burgers model can achieve higher accuracy in terms of the ability to fit the test data, which verifies the applicability of the fractal Burgers model to describe the creep characteristics of the soft soil layer. In addition, the fractal Burgers model applies a local operator that avoids a convolution integral, making it more computationally convenient and thus more applicable to practical problems.

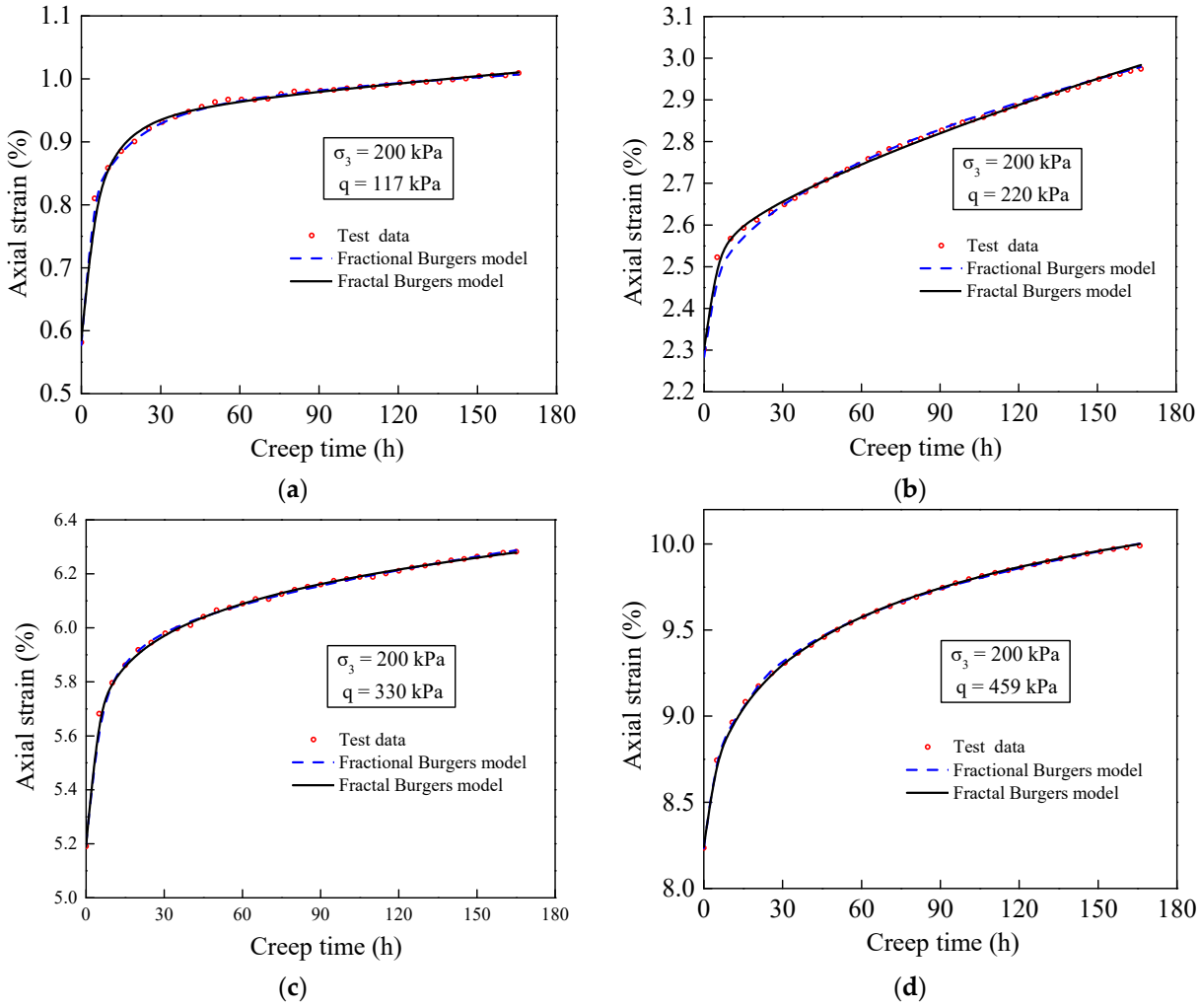

Figure 13. Comparison of test data with fractal Burgers and fractional Burgers models: (**a**) q = 117 kPa; (**b**) q = 220 kPa; (**c**) q = 330 kPa; (**d**) q = 459 kPa.

4.2. Model Comparison

The component models that are widely used to describe the elastoplastic creep characteristics of soft soil mainly include Merchant, traditional Burgers, five-element generalized Kelvin, and fractional Burgers models [26], which are composed of the most basic components connected by different connection methods, as shown in Figures 12 and 14, where E and η are Young's modulus and the viscosity coefficient, and the subscripts 0, 1 and 2 represent Hooke spring, the first Kelvin element and the second Kelvin element in a fractal form, respectively. To compare and analyze the fitting accuracy of different models, the fitting analyses of the test data using the corresponding constitutive models are shown in Figure 15. From the comparison, it can be seen that in the case of the same type of basic components, the greater the number of model components is, the higher the accuracy of the model fit, but the greater the computational workload. A comparison of the fractal Burgers and traditional Burgers models suggests that replacing the Newton dashpot with the fractal dashpot will achieve a higher fitting accuracy in the case of an equal number of components, and the calculation process is easy to implement.

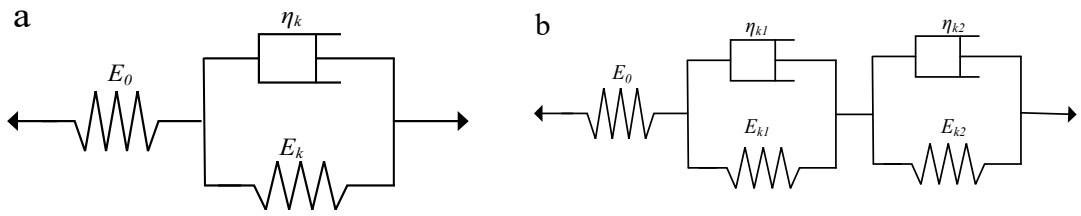

Figure 14. Schematic of different models: (**a**) Merchant model; (**b**) five-element generalized Kelvin model.

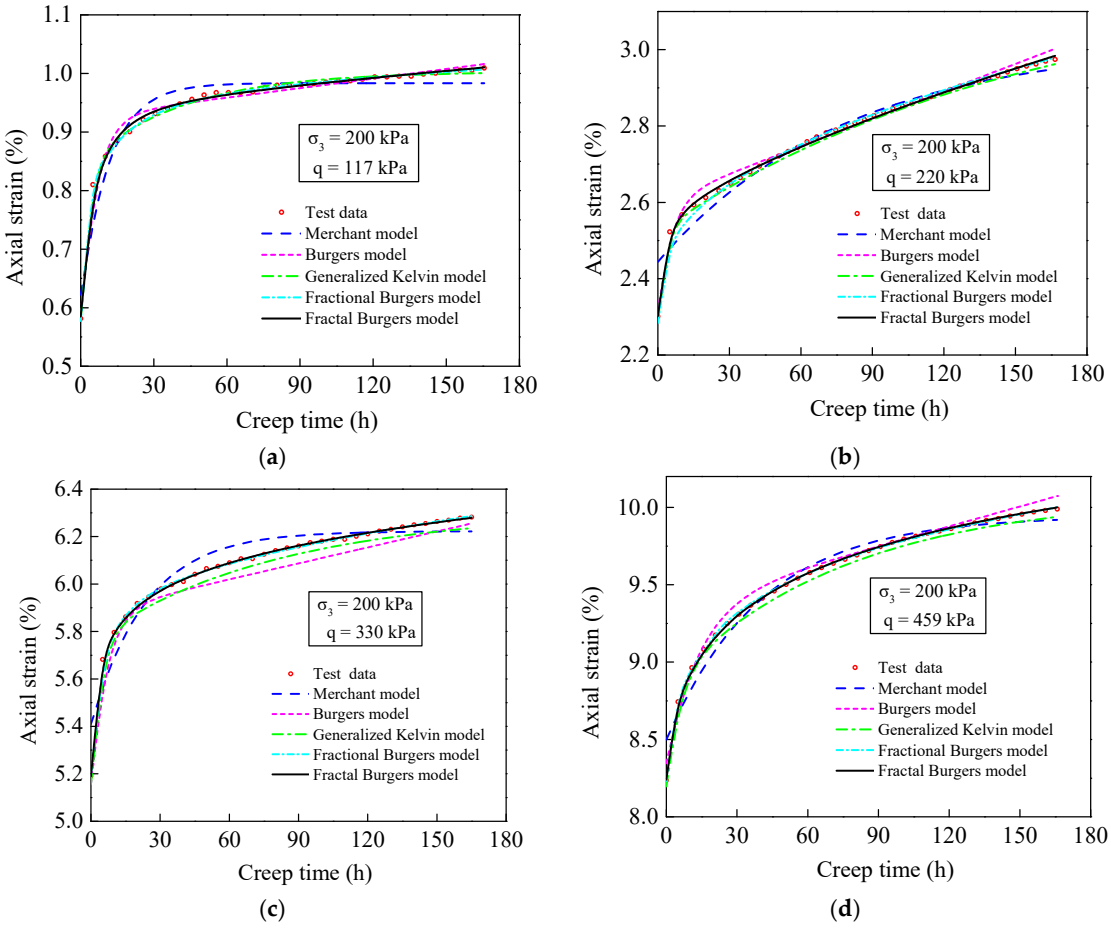

Figure 15. Comparison of test data and the fitting curves of different models: (**a**) q = 117 kPa; (**b**) q = 220 kPa; (**c**) q = 330 kPa; (**d**) q = 459 kPa.

Figure 15 also shows that the model fitting accuracy mainly depends on the curve slope and inflection point. This test involves only two stages of creep deformation: the initial curve slope determines the initial creep deformation, the final curve slope determines the long-term creep deformation value, and the inflection point determines the turning point of creep from one stage to another. Comparing the Merchant model and the Burgers model, it can be found that the Abel dashpot in the Maxwell model has a significant impact on the curve inflection point and slope. The Merchant model has an obvious inflection point delay, and the slope tends to zero with time going on, while the Burgers model exhibits the opposite phenomenon, which is not obvious in a short period but will become more pronounced in long-term observations. Comparing the traditional Burgers model with the fractal Burgers model, it can be found that the existence of derivative order β mainly plays a role in reducing the slope of the final curve. In general, the fitting laws of all the above models tend to be consistent with the test data, and the difference lies in the

degree of fitting coincidence. For low-stress soil, increasing the number of components can improve the fitting accuracy, while for high-stress soil, the fractional derivative and fractal derivative methods can effectively improve the fitting accuracy.

4.3. Fractal Burgers Model Parametric Sensitivity Analysis

The above analysis shows that the fractal Burgers model is suitable for describing the creep characteristics of soft soil. As seen from Equation (10), the parameters affecting the creep characteristics mainly include Young's modulus E, the viscosity coefficient η of the dashpot, the order of the fractal derivative β, and the stress level σ. To better analyze the influence of model parameters, according to the results of the abovementioned test and the fractal Burgers model fitting, taking 200 kPa confining pressure and 220 kPa deviatoric stress as an example, the fitting parameters of the proposed model are shown in Table 5, and the parameter sensitivity analysis is carried out for the creep model to clarify the influence mechanism of each parameter.

First, by changing Young's modulus of the Maxwell and Kelvin elements, the influence of Young's modulus on the creep curve is analyzed. As Figure 16a indicates, E_m has a negative linear correlation with the creep strain, which affects the initial transient elastic deformation, and E_k has a negative nonlinear correlation with the creep strain, affecting the creep rate and inflection point, and the effect is particularly pronounced when the creep strain is small.

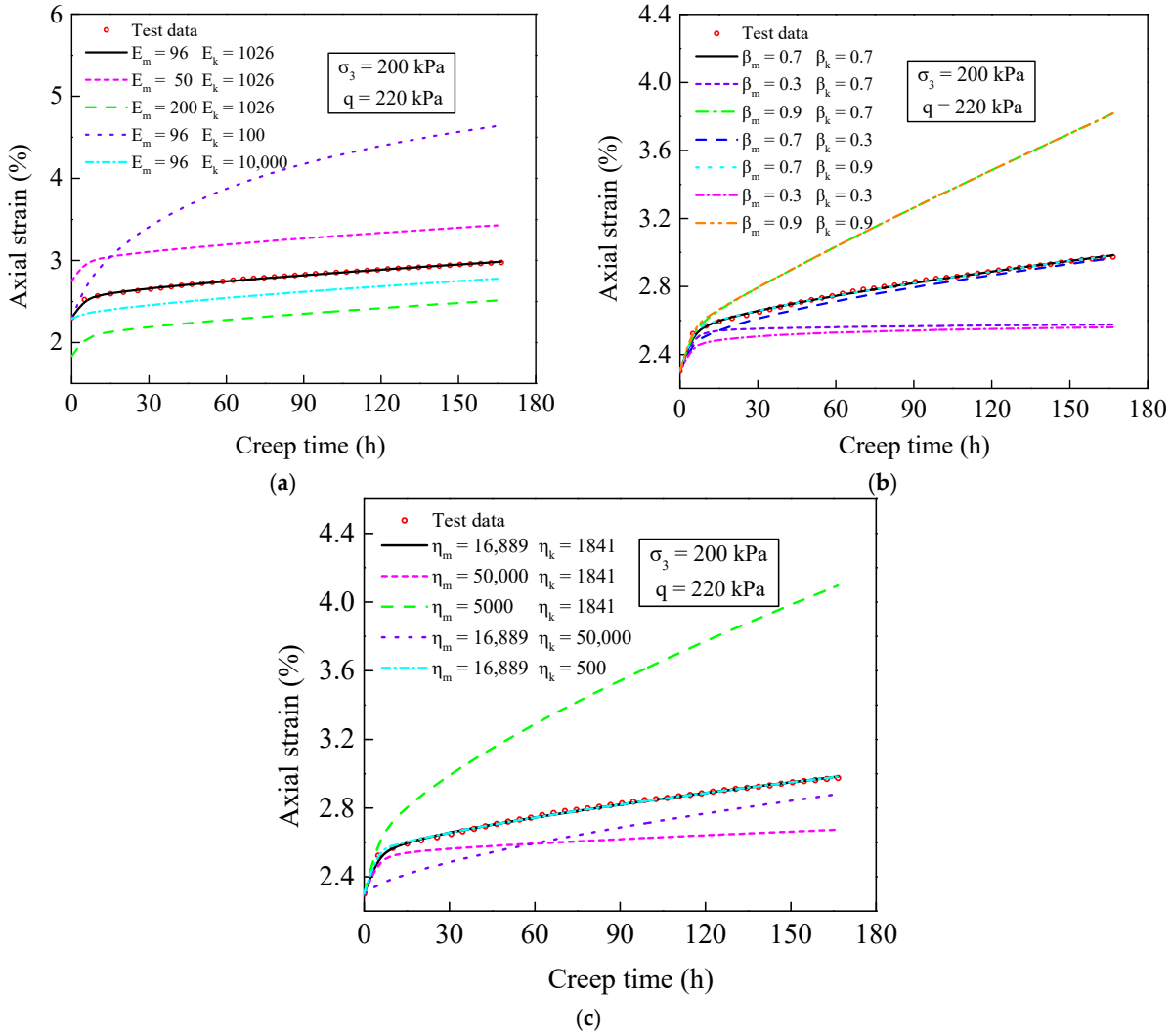

Figure 16. Sensitivity of the creep strain to different parameters: (**a**) Young's modulus; (**b**) derivative order; (**c**) viscosity coefficient.

The fractal Burgers model is characterized by the use of fractal derivative theory to solve the nonlinear creep problem, and the influence of the derivative order on the creep characteristics is significant. Leaving the other parameters unchanged and only changing the derivative order of the model, the rheological curves corresponding to the different derivative orders can be obtained, as shown in Figure 16b. The derivative order is positively correlated with the creep value and deformation rate, of which β_m significantly affects the creep rate, and β_k has an obvious impact on the inflection point of the creep curve. The presence of a derivative order causes the slope of the curve to appear to be linear.

To study the influence law of the viscosity coefficient parameters, creep curves can be obtained by changing the viscosity coefficient, as shown in Figure 16c. The viscosity coefficient is negatively correlated with the value and deformation rate of the creep, where η_m significantly affects the creep rate and η_k has a more significant influence on the inflection point of the creep curve; that is to say, η_k represents the speed rate when the deformation tends to be in steady state during the creep stage. A larger value of η_k indicates that the soil would take longer to reach the steady state. In addition, the presence of a viscosity coefficient makes the curve nonlinear.

The effect of the stress level σ can be directly observed from the test result in Figure 6, and the influence of the stress level on creep characteristics is significant. At the low-stress level, the creep deformation is mainly determined by the transient deformation value, while at the high-stress level, it is the result of the combination of transient creep values and steady-state strain rates. The higher the stress level is, the greater the creep deformation value.

According to the sensitivity analysis of the above key parameters, the creep rate is largely limited by the derivative order; the viscosity coefficient mainly affects the morphology of the curve, and Young's modulus and the stress level significantly affect the deformation value of the soil. For the two model elements in the fractal Burgers model, the Maxwell component-related parameters mainly affect the initial creep value and rate, and the Kelvin component mainly affects the creep curve inflection point and morphology. In fact, σ/E_m is an instantaneous elastic strain that can be recovered when unloaded; $\sigma/E_k(1-e^{\frac{-E_k}{\eta_k}t^\beta})$ is an elastic after-effect deformation that decays by a negative exponent, which is reflected in the first stage of the creep curve; σ/η_m is characterized as an unrecoverable strain of the steady-state strain rate and is embodied in the second stage of the creep curve. In general, creep characteristics are the result of the simultaneous combination of multiple elements and factors.

5. Discussions

The classical Burgers model and fractional Burgers model were improved by introducing the fractal dashpot, and the creep characteristics of the soft soil sampled from a riverside in Jiangsu were analyzed in combination with the test results. The proposed fractal Burgers model can accurately describe the creep characteristics of the soil, which verifies the applicability and convenience of describing the viscoelastic plastic characteristics of the soil with a fractal dashpot. However, the fractal derivative creep model mentioned in this paper is only a mathematical expression based on the fractal derivative, which is a preliminary result of the integer derivative of time [27]. As a relatively new component, the exact physical significance of fractal dashpot and the physical mechanisms of describing the model are still questions that need to be further studied.

The complete curve of the classical creep test consists of three stages: instantaneous creep, steady-state creep, and accelerated creep [32]. In the actual project, the failure deviatoric stress state usually does not occur, so the deviatoric stress state of the creep test is lower than the failure stress, and the creep curve mainly shows the creep characteristics of the first two stages [35,39]. By carrying out the failure deviatoric stress creep test of the soil, the characteristics of the three stages of creep can be further understood by considering the failure process [33]. In addition, the current traditional creep model is established under a specified constant stress level and confining pressure, and the model parameters are

determined by fitting the test data. However, the laboratory test samples are limited, and the influence of confining pressure and stress at any state on the creep model parameters are not quantified. How to deduce the creep model parameters related to any stress and confining pressure state through the limited data of the laboratory test will have higher practical research significance and value.

The laboratory creep test of the soil is generally carried out in a limited period of time (ranging from a few days to several months). The proposed creep model can well characterize the results of the short-term creep test, but the service period of the actual project is nearly 100 years, which belongs to long-term creep, and the geological conditions at the project site are complex—whether the proposed model can accurately characterize the long-term creep behavior and how to speculate the long-term creep behavior in the actual project through the laboratory test is a problem that needs future study. At present, there is an adopted method to build a numerical simulation model through the laboratory test and predict the long-term creep of the actual project [46], but more engineering measurement cases are still needed to verify it.

6. Conclusions

This paper establishes an improved fractal Burgers creep constitutive model based on the fractal derivative by replacing the Abel dashpot with a fractal dashpot in the fractional Burgers model, and an analytical solution is given. According to the fitting analysis of the results of the triaxial test, the relevant parameters in the model are determined, and sensitivity analyses of the parameters are further performed. The conclusions are as follows:

1. The analysis of the triaxial consolidation drainage test indicates that the stress level and confining pressure have a significant influence on the creep characteristics of the soil. Under the state where the stress level is lower than the failure stress, the creep strain curve presents a transient creep stage and a steady-state creep stage. The soil creep curves exhibit nonlinear viscoelasticity characteristics.
2. By validating the test data at different stress levels and confining pressures, the proposed fractal creep model has wide applicability for describing the transient and steady stages of soft soil based on triaxial creep tests. Compared with other creep models widely used in geotechnical materials, the proposed model can more accurately simulate the creep behavior of soil. This model has the advantages of fewer parameters and high accuracy.
3. Parameter sensitivity analysis has shown that creep characteristics are the result of the combined action of multiple elements and multiple factors at the same time. Among them, the fractal derivative order is the key factor controlling the strain rate. The viscosity coefficient mainly affects the nonlinear morphology of the curve, and the creep curve of different modes can be obtained by adjusting the derivative order and viscosity coefficient in the equation.

Author Contributions: Conceptualization, Q.Y., J.D., G.D., W.G., F.Z. and M.Z.; software, Q.Y.; validation, Q.Y.; formal analysis, Q.Y.; investigation, Q.Y.; resources, Q.Y.; data curation, Q.Y.; writing—original draft preparation, Q.Y.; writing—review and editing, J.D., G.D., W.G., M.Z. and F.Z.; visualization, Q.Y.; supervision, J.D., G.D. and W.G.; project administration, J.D., G.D. and W.G.; funding acquisition, J.D., G.D. and W.G. All authors have read and agreed to the published version of the manuscript.

Funding: This work was funded by the National Key Research and Development Program of China, project number 2021YFB1600300; the National Natural Science Foundation of China, project number 52178317, 52078128 and the Natural Science Foundation of Jiangsu Province, project number BK20200675. The authors are grateful for their support.

Institutional Review Board Statement: Not applicable.

Informed Consent Statement: Not applicable.

Data Availability Statement: The data presented in this study are available on request from the corresponding author. The data are not publicly available due to the nature of this research.

Conflicts of Interest: The authors declare no conflict of interest.

References

1. Zhu, S.; Yin, Y.; Li, B.; Wei, Y.J. Shear creep characteristics of weak carbonaceous shale in thick layered Permian limestone, southwestern China. *J. Earth Syst. Sci.* **2019**, *128*, 28. [CrossRef]
2. Miao, H.B.; Wang, G.H. Effects of clay content on the shear behaviors of sliding zone soil originating from muddy interlayers in the Three Gorges Reservoir, China. *Eng. Geol.* **2021**, *294*, 106380. [CrossRef]
3. Wang, S.; Wang, J.G.; Wu, W.; Cui, D.S.; Su, A.J.; Xiang, W. Creep properties of clastic soil in a reactivated slow-moving landslide in the Three Gorges Reservoir Region, China. *Eng. Geol.* **2020**, *267*, 105493. [CrossRef]
4. Miao, F.S.; Zhao, F.C.; Wu, Y.P.; Li, L.W.; Xue, Y.; Meng, J.J. A novel seepage device and ring-shear test on slip zone soils of landslide in the Three Gorges Reservoir area. *Eng. Geol.* **2022**, *307*, 106779. [CrossRef]
5. Yao, Y.P.; Huang, J.; Wang, N.D.; Luo, T.; Han, L.M. Prediction method of creep settlement considering abrupt factors. *Transp. Geotech.* **2020**, *22*, 100304. [CrossRef]
6. Ding, P.; Xu, R.Q.; Zhu, Y.H.; Wen, M.J. Fractional derivative modelling for rheological consolidation of multilayered soil under time-dependent loadings and continuous permeable boundary conditions. *Acta Geotech.* **2022**, *17*, 2287–2304. [CrossRef]
7. Jessen, J.; Cudmani, R. Rate- and Time-Dependent Mechanical Behavior of Foam-Grouted Coarse-Grained Soils. *J. Geotech. Geoenvironmental Eng.* **2022**, *148*, 04022022. [CrossRef]
8. Oliveira, P.J.V.; Santos, S.L.; Correia, A.A.S.; Lemos, L.J.L. Numerical prediction of the creep behaviour of an embankment built on soft soils subjected to preloading. *Comput. Geotech.* **2019**, *114*, 103140. [CrossRef]
9. Sun, Y.; Gao, Y.; Shen, Y. Mathematical aspect of the state-dependent stress-dilatancy of granular soil under triaxial loading. *Géotechnique* **2019**, *69*, 158–165. [CrossRef]
10. Li, D.W.; Zhang, C.C.; Ding, G.S.; Zhang, H.; Chen, J.H.; Cui, H.; Pei, W.S.; Wang, S.F.; An, L.S.; Li, P.; et al. Fractional derivative-based creep constitutive model of deep artificial frozen soil. *Cold Reg. Sci. Technol.* **2020**, *170*, 102942. [CrossRef]
11. Singh, A.; Mitchell, J.K. General stress-strain-time function for soils. *J. Soil Mech. Found Eng. Div.* **1968**, *94*, 21–46. [CrossRef]
12. Mesri, G.; Febres-Cordero, E.; Shields, D.R.; Castro, A. Shear stress –strain-time behaviour of clays. *Géotechnique* **1981**, *31*, 537–552. [CrossRef]
13. Schiessel, H.; Metzler, R.; Blumen, A.; Nonnenmacher, T.F. Generalized viscoelastic models: Their fractional equations with solutions. *J. Phys. A Math. Gen.* **1995**, *28*, 65–67. [CrossRef]
14. Sun, J. *Rheology of Geotechnical Materials and Its Engineering Application*; China Construction Industry Press: Beijing, China, 1999.
15. Nishihara, M. Rheological properties of rocks I and II. *Doshisha Eng. Rev.* **1958**, *8*, 32–35, 85–115.
16. Hou, F.; Lai, Y.M.; Liu, E.L.; Luo, H.W.; Liu, X.Y. A creep constitutive model for frozen soils with different contents of coarse grains. *Cold Reg. Sci. Technol.* **2018**, *145*, 119–126. [CrossRef]
17. Zhang, Z.L.; Wang, T. On creep behavior of mudstone in the Tianshui area, China. *Bull. Eng. Geol. Environ.* **2022**, *81*, 321. [CrossRef]
18. Ye, J.H.; Haiyilati, Y.; Cao, M.; Zuo, D.J.; Chai, X.W. Creep characteristics of calcareous coral sand in the South China Sea. *Acta Geotech.* **2022**, *148*, 04022022. [CrossRef]
19. Tian, X.W.; Xiao, H.B.; Li, Z.Y.; Su, H.Y.; Ouyang, Q.W.; Luo, S.P.; Yu, X.P. A Fractional Order Creep Damage Model for Microbially Improved Expansive Soils. *Front. Earth Sci.* **2022**, *10*, 942844. [CrossRef]
20. Xu, B.X.; Cui, Z.D. Investigation of a fractional derivative creep model of clay and its numerical implementation. *Comput. Geotech.* **2020**, *119*, 103387. [CrossRef]
21. Xiang, G.J.; Yin, D.S.; Cao, C.X.; Gao, Y.F. Creep modelling of soft soil based on the fractional flow rule: Simulation and parameter study. *Appl. Math. Comput.* **2021**, *403*, 126190. [CrossRef]
22. Liang, Y.J.; Guan, P.Y. Improved Maxwell model with structural dashpot for characterization of ultraslow creep in concrete. *Constr. Build. Mater.* **2022**, *329*, 127181. [CrossRef]
23. Wu, F.; Zhou, X.H.; Ying, P.; Li, C.B.; Zhu, Z.M.; Chen, J. A Study of Uniaxial Acoustic Emission Creep of Salt Rock Based on Improved Fractional-Order Derivative. *Rock Mech. Rock Eng.* **2022**, *55*, 1619–1631. [CrossRef]
24. Zhang, L.; Zhou, H.W.; Wang, X.Y.; Wang, L.; Su, T.; Wei, Q.; Deng, T.F. A triaxial creep model for deep coal considering temperature effect based on fractional derivative. *Acta Geotech.* **2022**, *17*, 1739–1751. [CrossRef]
25. Liao, M.K.; Lai, Y.M.; Liu, E.L.; Wan, X.S. A fractional order creep constitutive model of warm frozen silt. *Acta Geotech.* **2017**, *12*, 377–389. [CrossRef]
26. Zhang, Z.; Huang, C.J.; Jin, H.J.; Feng, W.J.; Jin, D.D.; Zhang, G.K. A creep model for frozen soil based on the fractional Kelvin–Voigt's model. *Acta Geotech.* **2022**, *271*, 1–17. [CrossRef]
27. Cai, W.; Chen, W.; Xu, W.X. Characterizing the creep of viscoelastic materials by fractal derivative models. *Int. J. Non-Linear Mech.* **2016**, *87*, 58–63. [CrossRef]

28. Liang, Y.J.; Ye, A.Q.; Chen, W.; Gatto, R.G.; Colon-Perez, L.; Mareci, T.H.; Magin, R.L. A fractal derivative model for the characterization of anomalous diffusion in magnetic resonance imaging. *Commun. Nonlinear Sci. Numer. Simul.* **2016**, *39*, 529–537. [CrossRef]
29. Reyes-Marambio, J.; Moser, F.; Gana, F.; Seveion, B.; Calderom-Muno, W.R.; Palma-Behnke, R.; Estevez, P.A.; Orchard, M.; Cortes, M. A fractal time thermal model for predicting the surface temperature of air-cooled cylindrical Li-ion cells based on experimental measurements. *J. Power Sources* **2016**, *306*, 636–645. [CrossRef]
30. Mashayekhi, S.; Hussaini, M.Y.; Oates, W. A physical interpretation of fractional viscoelasticity based on the fractal structure of media: Theory and experimental validation. *J. Mech. Phys. Solids* **2019**, *128*, 137–150. [CrossRef]
31. Su, X.L.; Chen, W.; Xu, W. Characterizing the rheological behaviors of non-Newtonian fluid via a viscoelastic component: Fractal dashpot. *Adv. Mech. Eng.* **2017**, *9*, 968738. [CrossRef]
32. Wang, R.; Zhou, Z.; Zhou, H.W.; Liu, J.F. A fractal derivative constitutive model for three stages in granite creep. *Results Phys.* **2017**, *7*, 2632–2638. [CrossRef]
33. Yao, W.M.; Hu, B.; Zhan, H.B.; Ma, C.; Zhao, N.H. A novel unsteady fractal derivative creep model for soft interlayers with varying water contents. *KSCE J. Civ. Eng.* **2019**, *23*, 5064–5075. [CrossRef]
34. Kabwe, E.; Karakus, M.; Chanda, E.K. Isotropic damage constitutive model for time-dependent behaviour of tunnels in squeezing ground. *Comput. Geotech.* **2020**, *127*, 103738. [CrossRef]
35. Gao, L.C.; Dai, G.L.; Wan, Z.H.; Zhu, M.X.; Zhu, W.B. Prediction of triaxial drained creep behaviors of interactive marine-terrestrial deposit soils by fractal derivative. *Eur. J. Environ. Civ. Eng.* **2022**, *26*, 3065–3078. [CrossRef]
36. *GB 50021-2001*; Code for Investigation of Geotechnical Engineering. China Architecture Publishing & Media Co., Ltd.: Beijing, China, 2001.
37. *GB/T 50123-2019*; Standard for Soil Test Method. China Planning Press: Beijing, China, 2019.
38. Yuan, J.Y.; Xu, C.; Zhao, C.F.; He, Z.M.; Gao, Y.B.; Su, X.; Chen, B.; Wei, D.D. *Geotechnical Test and In-Situ Test*; Tongji University Press: Shanghai, China, 2004.
39. Deng, H.Y.; Dai, G.L.; Qiu, G.Y.; Chen, Z.S.; Lin, X. Drained creep test and component creep model of soft silty clay in Hangzhou Bay. *J. Southeast Univ. Nat. Sci. Ed.* **2021**, *51*, 318–324.
40. Kong, L.W.; Zhang, X.W.; Guo, A.G.; Cai, Y. Creep behavior of Zhanjiang strong structured clay by drained triaxial test. *Chin. J. Rock Mech. Eng.* **2011**, *30*, 365–372.
41. Zhao, D.; Gao, Q.F.; Hattab, M.; Hicher, P.Y.; Yin, Z.Y. Microstructural evolution of remolded clay related to creep. *Transp. Geotech.* **2020**, *24*, 100367. [CrossRef]
42. Podlubny, I. *Fractional Differential Equations*; Academic Press: San Diego, CA, USA; London, UK, 1999.
43. Zhou, H.W.; Wang, C.P.; Mishnaevsky, L.; Duan, Z.Q.; Ding, J.Y. A fractional derivative approach to full creep regions in salt rock. *Mech. Time-Depend. Mater.* **2013**, *17*, 413–425. [CrossRef]
44. Bateman, H.; Erdelyi, A. *Higher Transcendental Functions*; McGraw-Hill Company: New York, NY, USA, 1953.
45. Zhang, C.C.; Zhu, H.H.; Shi, B.; Liu, L.C. Theoretical investigation of interaction between a rectangular plate and fractional viscoelastic foundation. *J. Rock Mech. Geotech. Eng.* **2015**, *45*, 324–335. [CrossRef]
46. Yuan, Y.; Liu, R.; Qiu, C.L.; Tan, R.J. Establishment and Application of Creep Constitutive Model Related to Stress Level of Soft Soil. *J. Tianjin Univ.* **2018**, *51*, 711–719.